Assessment of k-ε / EASM Turbulence Model Upgrades for Analyzing High Speed Aeropropulsive Flows

H. Ayyalasomayajula[†], D.C. Kenzakowski[‡], J.L. Papp[†], and S.M. Dash[±]
Combustion Research and Flow Technology, Inc. (CRAFT Tech)
6210 Keller's Church Road, Pipersville, PA 18947
haritha@craft-tech.com
Phone: 215-766-1520 / Fax: 215-766-1524

This paper discusses the numerical simulations of selected high-speed aeropropulsive applications including axisymmetric supersonic base flowfields, with and without jets, and three-dimensional supersonic hot jets. Comparisons are made using a compressibility corrected k-ε turbulence model and an Explicit Algebraic Stress Model (EASM). The present EASM, referred to as EASM/J, has been modified to correctly predict the mixing of basic jet and free shear flows. A structured, parallel, finite-volume, Navier Stokes code, CRAFT CFD is used as the flow solver. In the present study, the EASM/J analysis assumes a fixed (equilibrium) value of production-to-dissipation ratio. The effect of the compressibility correction as implemented in CRAFT CFD, in predicting the flow reattachment location and base pressure distribution is investigated. For base region studies, the k-ε and EASM/J models predict comparable results, but base pressure distributions are closer to the experimental data without using the compressibility correction. For the jet with base study, the predictions with and without the correction bound the data. For the three-dimensional cases, there is no substantive difference in mean flow predictions using k-ε and EASM/J.

Nomenclature

u_i = Cartesian components of velocity
t = time
ρ = density
μ_L = laminar viscosity
τ_{ij} = shear stress tensor
k = turbulent kinetic energy
ε = turbulent dissipation rate
μ_T = turbulent eddy viscosity
P/ε = ratio of production of turbulent kinetic energy to turbulent dissipation rate
b_{ij} = anisotropy stress tensor
S_{ij} = strain-rate tensor
W_{ij} = rotation rate tensor
a_i = coefficients calculated in EASM/J
D = the combined effect of turbulent transport and viscous diffusion

43rd Aerospace Sciences Meeting and Exhibit, Jan. 10-13, 2005, Reno, Nevada.

[†]Research Scientist, AIAA Member.
[‡]Senior Research Scientist, AIAA Member.
[±]President and Chief Scientist, Associate Fellow AIAA.

Report Documentation Page

Form Approved
OMB No. 0704-0188

1. REPORT DATE	2. REPORT TYPE	3. DATES COVERED
2005		**00-00-2005 to 00-00-2005**

4. TITLE AND SUBTITLE	5a. CONTRACT NUMBER
Assessment of k-e/EASM Turbulence Model Upgrades for Analyzing High Speed Aeropropulsive Flows	5b. GRANT NUMBER
	5c. PROGRAM ELEMENT NUMBER
6. AUTHOR(S)	5d. PROJECT NUMBER
	5e. TASK NUMBER
	5f. WORK UNIT NUMBER
7. PERFORMING ORGANIZATION NAME(S) AND ADDRESS(ES) **Combustion Research and Flow Technology Inc (CRAFT Tech),6210 Keller's Church Road,Pipersville,PA,18947**	8. PERFORMING ORGANIZATION REPORT NUMBER
9. SPONSORING/MONITORING AGENCY NAME(S) AND ADDRESS(ES)	10. SPONSOR/MONITOR'S ACRONYM(S)
	11. SPONSOR/MONITOR'S REPORT NUMBER(S)

12. DISTRIBUTION/AVAILABILITY STATEMENT
Approved for public release; distribution unlimited

13. SUPPLEMENTARY NOTES
The original document contains color images.

14. ABSTRACT

15. SUBJECT TERMS

16. SECURITY CLASSIFICATION OF:			17. LIMITATION OF ABSTRACT	18. NUMBER OF PAGES	19a. NAME OF RESPONSIBLE PERSON
a. REPORT	b. ABSTRACT	c. THIS PAGE			
unclassified	**unclassified**	**unclassified**		**14**	

Standard Form 298 (Rev. 8-98)
Prescribed by ANSI Std Z39-18

I. Introduction

This paper compares the performance of an aero-propulsive variant of the EASM turbulence model [2,3], to that of the k-ε turbulence model [4] used in our jet and aeropropulsive studies, for a series of test cases of increasing complexity. The k-ε model uses the original Launder et al. [5] coefficients and contains a compressibility-correction [4] found to adequately analyze a variety of basic high-speed jets and free shear flows. The EASM utilizes this k-ε model for obtaining needed turbulent kinetic energy and time-scale information and makes use of a recalibrated pressure-strain correlation coefficient to perform comparably to the k-ε model for basic jet and free shear flow mixing [2,3].

EASM models have several potential advantages over k-ε models that include realizability (in a more fundamental framework than achieved via just adding realizability modifications to k-ε) and a better prediction of turbulent stresses, in particular normal stress anisotropy. As we move from simple jets and free shear flows, in this paper we examine what improvements over k-ε model are afforded by EASM for a variety of more complex aeropropulsive flows. This paper deals with issues of flow structure as exhibited by the improved behavior with EASM for a missile at angle-of-attack with cross-flow separation (Figure 1). Issues of anisotropy, as related to jet noise problems, are the subject of a related paper at this meeting [6]. We have used the basic ε-equation in all these studies, realizing that extended variants will be needed for complex flows with curvature, swirl, etc., but reserving the exploration of such corrections for a future paper. Both the k-ε and EASM models have low-Re and wall function capabilities to treat near-wall regions, and the overall equations will be described in the Section III. Specific problems that have been analyzed include that of:

1. Base region behind a cylinder[7];
2. Propulsive jet into a moving stream with a large base [8];
3. Lateral slot jet injection [9];
4. Propulsive jet with lobes in the exhaust; and,
5. Dual supersonic interacting jets.

The authors and coworkers have been involved in the extension and unification of turbulence models for application to a broad variety of aero-propulsive flows ranging from laboratory jets and aircraft exhausts, to scramjet combustors and rocket plumes [10,11,12]. Thermal/species turbulent transport issues can be quite significant in aeropropulsive flows, and are also the subject of a related paper at this meeting[13].

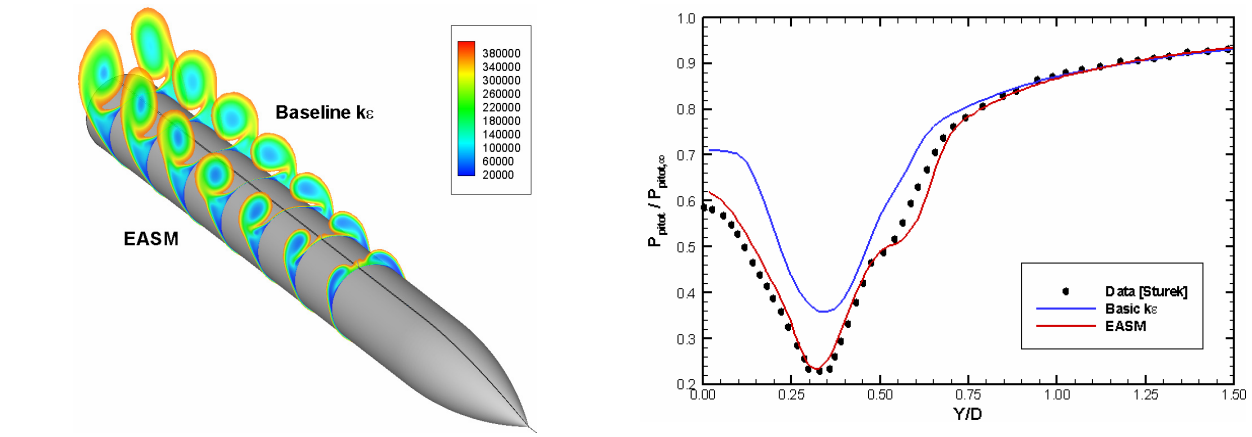

(a). Comparison of stagnation pressure contours at selected stations along missile at α=14-deg [1].

(b). Predicted pitot pressure improvements at X/D=11.5 with EASM [1].

Figure 1.

II. Background

Most turbulence models within a RANS framework are linear eddy viscosity models, which assume the Boussinesq hypothesis to be valid. For some of the complex turbulent flows of engineering importance, this assumption may fail. Full Reynolds stress models are more accurate for modeling such flows as they do not assume the turbulent shear stresses to be proportional to the rate of mean strain, and thus can be expected to provide better predictions for flows with sudden changes in the mean strain rate, or with effects such as streamline curvature. However, keeping in view the computational effort needed to implement these models, a more practical approach, is

that of using Algebraic Stress Models (ASM). Unlike full Reynolds Stress Models, which require solving the full partial differential equations for each of the stresses, Algebraic Stress Models provide a nonlinear relationship between the Reynolds stresses and the mean rate of strain. Several researchers developed these nonlinear relationships in the form of a series expansion having the Boussinesq assumption as the leading term. Early studies by Rodi [14] deduced the nonlinear algebraic equation for the Reynolds stresses by simplifying the full Reynolds stress partial differential equation (PDE). Algebraic Stress Models are derived from the full Reynolds stress transport equation, and hence are expected to perform better in predicting the flow physics. Initial attempts to solve ASM equations implicitly limited the allowable time step size to obtain a stable solution, particularly for complex flows. Pope [15] developed a procedure for obtaining explicit solution to the proposed nonlinear algebraic equation for two-dimensional mean flows. Gatski and Speziale [16] came up with a similar method for three-dimensional flows. In the present EASM model however, the approach of Jongen and Gatski [17,18] for two-dimensional flows is used, and applied for complex aeropropulsive applications. A brief overview of the turbulence models used for current research is provided in the following two sections.

III. Overview of Unified Variant of k-ε Model

The governing equations are Favré averaged (mass averaged) Navier-Stokes equations. The closure to the Favré averaged Navier-Stokes equations is achieved by relating the Reynolds stresses to available mean flow gradients, such as in the Boussinesq approximation. This requires specification of turbulent eddy viscosity, which presently is determined using the k-ε equations. The transport equation for turbulent kinetic energy is given by,

$$\frac{\partial \rho k}{\partial t} + \rho u_j \frac{\partial k}{\partial x_j} - \frac{\partial}{\partial x_j}\left[\left(\mu + \frac{\mu_T}{\sigma_k}\right)\frac{\partial \rho k}{\partial x_j}\right] = \tau_{ij}\frac{\partial u_i}{\partial x_j} - \rho\varepsilon + SS_k \tag{1}$$

and the transport equation for dissipation rate equation is given by,

$$\frac{\partial \rho \varepsilon}{\partial t} + \rho u_j \frac{\partial \varepsilon}{\partial x_j} - \frac{\partial}{\partial x_j}\left[\left(\mu + \frac{\mu_T}{\sigma_\varepsilon}\right)\frac{\partial \rho \varepsilon}{\partial x_j}\right] = C_{\varepsilon_1}\tau_{ij}\frac{\partial u_i}{\partial x_j}\frac{\varepsilon}{k} - C_{\varepsilon_2}\rho\varepsilon\frac{\varepsilon}{k} + SS_\varepsilon \tag{2}$$

where $\mu_T = C_\mu \rho \frac{k^2}{\varepsilon}$, and the coefficients used in the model are $C_{\varepsilon_1} = 1.43$, $C_{\varepsilon_2} = 1.92$, $C_\mu = 0.09$, $\sigma_k = 1.0$, and $\sigma_\varepsilon = 1.3$. SS_k is the modeled pressure dilatation term, which accounts for reduced mixing in compressible turbulent flows. The present approach is a combination of the Sarkar[19] model, and Zeman [20,21] model. The functioning of Sarkar[19] model in a compressible flow is through the dilatational and pressure fluctuation terms. The original Sarkar model involves correction at all levels of compressibility. For lower speed compressible mixing layers, this produces unwanted mixing reductions and smaller than experimentally measured growth rates. The Zeman correction introduces a lag wherein the turbulence fluctuation due to compressibility must reach a certain threshold before affecting the dissipation. However, the original model of Zeman does not account for the additional effect of pressure dilatation. The current method combines the pressure dilatation of Sarkar with the lag concept of Zeman to reduce compressibility effects for low speed compressible flows [4]. For clarity, a short description about the working of each model is provided here before explaining the present method. The original Sarkar correction, which accounts for dilatational and pressure dilatational effects, is given as

$$\overline{u'_{i,i}} + \overline{p'u'_{i,i}} = -\alpha_2 M_T P_k - (\alpha_1 - \alpha_3) M_T^2 \ \rho\varepsilon \tag{3}$$

where $\alpha_1 = 0.5$, $\alpha_2 = 0.4$, $\alpha_3 = 0.2$. This correction was observed to introduce excessive dissipation and growth rate reduction at lower Mach numbers. To minimize this effect at low levels of compressibility, Zeman introduced a lag term, which eliminates the effect of compressibility correction term at low Mach numbers.

$$\tilde{M}_T = \max(M_T - \lambda, 0) \tag{4}$$

where λ is an appropriately chosen lag value to eliminate the effect of compressibility for lower Mach number jets. Introduction of $\tilde{M}_T$ required recalibrating α_i coefficients; and the final compressibility correction (c.c.) in the present model is given by,

$$SS_k = -\alpha_1 \tilde{M}_T^2 P_k - \alpha_2 \tilde{M}_T^2 \rho\varepsilon \tag{5}$$

where $\alpha_1 = 2.5$, $\alpha_2 = 2.0$, $\lambda = 0.2$. The compressibility correction has been validated for a range of basic flows at low and high Mach numbers [4]. However, some deficiencies associated with the use of this correction were found for complex aerpropulsive flows, and results obtained with and without using this correction will be discussed in Sec. V. The coefficients used in the turbulence model are applicable for high-Re flows, and modifications are necessary for improved prediction of the flow in the vicinity of a wall. The next subsection discusses the near-wall model used in the present analysis.

A. Near-wall Model

Several criteria need to be satisfied when choosing a near wall extension such that it is compatible with the high-Re k-ε model. In CRAFT CFD®, a modified version of So, Sarkar, Gerodimos, and Zhang (SSGZ) model [22] is employed. The damping coefficients used in the original SSGZ model have been modified to blend with the high-Re k-ε model, and the resulting changes to terms in the turbulent dissipation rate transport equation, given by Eqn. (2), are provided here. The first term in the RHS of Eqn. (2), representing production of dissipation is modified to

$$C_{\varepsilon_1} f_p \tau_{ij} \frac{\partial u_i}{\partial x_j} \frac{\varepsilon}{k} \tag{6}$$

where

$$f_p = 1 - \exp\left[-\left(\frac{\mathrm{Re}_T^2}{40}\right)\right] + \frac{0.24}{\cosh\left[1.0\left(\ln\left(\frac{\mathrm{Re}_y}{100}\right)\right)\right]} \tag{7}$$

The second term in the RHS of Eqn. (2), representing destruction of dissipation is modified to

$$C_{\varepsilon_2}\left[f_\varepsilon \rho\varepsilon \frac{\varepsilon}{k} - \frac{14}{9}\mu \frac{\partial\sqrt{k}}{\partial x_i}\frac{\partial\sqrt{k}}{\partial x_i}\right] \tag{8}$$

where

$$f_\varepsilon = 1 - \frac{2}{9}\exp\left(-\mathrm{Re}_T^2\right) \tag{9}$$

Finally, the coefficient of turbulent eddy viscosity is modified to

$$\mu_T = C_\mu f_\mu \rho \frac{k^2}{\varepsilon} \tag{10}$$

where

$$f_\mu = \left(1 + \frac{4}{\mathrm{Re}_T^{3/4}}\right)\tanh\left(\frac{\mathrm{Re}_y}{125}\right) \tag{11}$$

In the above equations, $\mathrm{Re}_T = \frac{\rho k^2}{\mu_L \varepsilon}$, is the turbulent Reynolds number, and $\mathrm{Re}_y = \frac{\rho\sqrt{k}}{\mu_L} y$, is wall-distance based Reynolds number. The k-ε turbulence model discussed above assumes a Boussinesq relation to relate the Reynolds stresses to the mean rate strain. EASM/J, which uses a nonlinear relationship between the Reynolds stresses and the mean rate of strain, is discussed in the next section.

IV. A Brief Overview of EASM Model

Derived from the Reynolds stress transport equation, the equation for Reynolds stress anisotropy tensor is given by,

$$\frac{Db_{ij}}{Dt} - \frac{1}{2k}\left(D_{ij} - \frac{\tau_{ij}}{k}D\right) = -\left[\frac{b_{ij}}{a_4} + \left(b_{ik}S_{kj} + S_{ik}b_{kj} - \frac{2}{3}b_{mn}S_{mn}\delta_{ij}\right) - a_2\left(b_{ik}W_{kj} - W_{ik}b_{kj}\right) + a_1 S_{ij}\right] \tag{12}$$

The coefficients a_i are directly related to the pressure-strain correlation model by $a_1 = \frac{1}{2}\left(\frac{4}{3} - C_2\right)$, $a_2 = \frac{1}{2}\left(2 - C_4\right)$, $a_3 = \frac{1}{2}\left(2 - C_3\right)$, $a_4 = g\tau$, where $C_2 = 0.36$, $C_3 = 1.25$, $C_4 = 0.4$, τ is the turbulence time scale, k/ε. Obtaining an explicit expression for the anisotropy tensor involves certain assumptions to LHS of Eqn. (12), and it is explained in the next few lines. An implicit solution for the above Reynolds stress tensor anisotropy equation, given in Eqn. (12) is obtained by assuming weak equilibrium condition on the turbulent stress anisotropy first proposed by Rodi [14]. This is expressed as,

$$\frac{Db_{ij}}{Dt} = 0 \tag{13}$$

and a second assumption is made, which considers anisotropy of the turbulence transport and viscous diffusion is proportional to the anisotropy of Reynolds stresses,

$$D_{ij} = \frac{\tau_{ij} D}{k} \tag{14}$$

Substituting Eq. (13) and Eq. (14) in Eq. (12), we obtain a locally implicit expression for the anisotropy tensor. Following the work of Jongen and Gatski [17], an explicit representation of the anisotropy tensor can be written as follows.

$$\boldsymbol{b} = \alpha_1 \boldsymbol{S} + \alpha_2\left(\boldsymbol{SW} - \boldsymbol{WS}\right) + \alpha_3\left(\boldsymbol{S}^2 - \frac{1}{3}\left\{\boldsymbol{S}^2\right\}\boldsymbol{I}\right) \tag{15}$$

The term g , which is required for calculating coefficient a_4 is written as follows:

$$g = \left[\left(\frac{C_1^1}{2} + 1\right)\frac{P}{\varepsilon} + \frac{C_1^0}{2} - 1\right]^{-1} \tag{16}$$

Speziale and Gatski [16] determined a fixed value for this expression, using homogeneous turbulence considerations. Direct application of this formulation can be problematic in the freestream, and requires regularization. Alternately, the variable production to dissipation ratio (P/ε) model in the EASM has been developed further such that non-linearity is accounted for in the calculation of coefficient g due to its dependence on (P/ε). The expression for g is given as:

$$g = \left[\left(1 + \frac{C_1^1}{2} \right) \left(\frac{P}{\varepsilon} + \frac{2}{3} \frac{\partial u_k}{\partial x_k} \tau \right) + \left(\frac{C_1^0}{2} - 1 \right) + \frac{P}{\varepsilon}\bigg|_\infty - \frac{P}{\varepsilon} \right]^{-1} \tag{17}$$

Further details of the EASM formulation are provided in Ref. 16.

V. Computational Methodology

The governing Navier-Stokes equations are solved using CRAFT CFD® flow solver. CRAFT CFD® is a three-dimensional, Navier-Stokes, finite-volume, structured, parallel, Fortran90 code, with several features available to handle complex flows. For time integration, implicit, ADI, up to second-order accuracy with Newton sub-iterations is available. Also, LU factorization method and fourth-order Runge Kutta explicit scheme can be used for approximating the temporal derivatives. For RANS applications, a second-order accurate upwind scheme is used for spatial discretization. A Roe flux splitting difference scheme is used for the treatment of inviscid fluxes. The grid blanking feature in CRAFT CFD® facilitates the placement of boundaries away from regions with large flow gradients. Also, a physical boundary in the flow field need not be a block boundary, using this grid blanking methodology. A domain decomposition procedure is employed for dividing the entire computational grid into specified number of processors, and the inter-processor communication is facilitated through MPI-based parallelization strategy.

VI. High Speed Aeropropulsive Applications

The results obtained in studying the selected aeropropulsive flows mentioned in Section I is discussed here. Also, more generalized flow physics will be emphasized using the EASM model, particularly for flows with substantive streamwise vorticity where the k-ε model has known deficiencies. This section is divided into five sub-sections, each discussing the flow analysis using k-ε , and EASM/J models for a specific application.

A. Base Region Study

Flow over axisymmetric step with a freestream Mach number 2.5 has been studied in detail. In this section, we discuss results obtained using both k-ε and EASM/J models compared with the experimental data of Herrin and Dutton[7]. This particular case was investigated by many researchers to gain a better understanding of the complex flow behavior, which involves flow separation, shear layer development, flow reattachment, recompression shock etc. A schematic of these fluid dynamic processes is shown in Fig. 2(a). The diameter of the cylinder (i.e. step height) is 63.5 mm, and the reader is referred to Ref.6 for the details of experimental set-up.

The approach boundary layer profile 1mm upstream of the step is generated by simulating the upstream supersonic flow at freestream Mach number 2.5. At the inflow boundary, flow variables p, V, and T are computed from the experimental stagnation conditions, P_o = 515kPa, and T_o = 294K. A Parabolized Navier-Stokes approach is used for performing the upstream boundary layer simulation. For the axisymmetric step case, no-slip conditions are prescribed on the step surface. Non-reflecting boundary condition is specified on the outflow boundary, where the flow variables are extrapolated from the interior by letting the first-order derivatives of all the flow variables normal to the boundary to vanish. Figure 2(b) shows the single-block grid generated, and Fig. 2(c) shows the Mach contours obtained using k-ε model, without compressibility correction (c.c.). Figure 2(d) shows the comparison of the ratio of mean axial velocity to freestream velocity distribution. The effect of compressibility correction, discussed in Section III, on the flow features has been studied. Higher base pressure is predicted using the compressibility correction as shown in Fig. 2(e), and the flow doesn't turn down as much. EASM/J and k-ε model predict comparable results with and without compressibility correction. The functioning of compressibility correction is being investigated further, with the possible need to use modified forms of the epsilon equation, or rapid strain modifications to the compressibility correction term.

B. Propulsive Jet with Base Region Study

Considering a more general configuration for study of the base region in a propulsive flow, a case of Petrie and Walker has been studied by Papp et al.[23]. The experiments are performed for a missile configuration, with a cylindrical afterbody and a propulsive jet in a Mach 1.4 free stream flow. The flow conditions are P_∞, = 42.316 kPa, T_∞ = 259.6K, P_{oj} = 2121.516kPa, T_{oj} = 361.48K. The flow involves important features like rapid expansion at the base corner, occurrence of Mach disk downstream of the base etc. A grid adaptive study has been performed as a part of the analysis to adequately resolve the Mach disk behind the base. Figure 3(a) shows the contours of

temperature. The base pressure distribution obtained with and without the compressibility correction, using the k-ε model are shown in Fig. 3(b). Similar to the observations made for the axisymmetric step flow in Sec VI-A, a higher base pressure is predicted when the compressibility correction is used. With c.c., k-ε and EASM/J models results are compared, and they match closely. Our base region results show that when a boundary layer goes through a rapid corner expansion, compressibility effects are over estimated using the c.c. model of Papp and Dash[4], which was calibrated for balanced pressure round jets and simple shear layers. The use of EASM produces results comparable to those of k-ε and does not improve the simulation. However, for other complex flows such as the lateral jet discussed below, the compressibility correction works well and provides marked improvements.

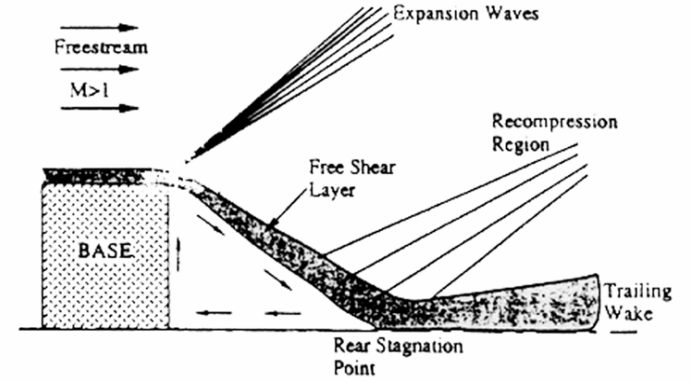

(a) Schematic of supersonic flow over axisymmetric step[7].

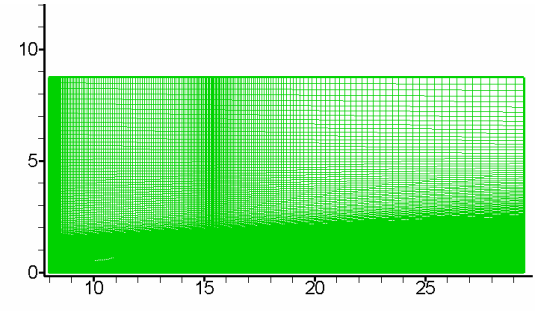

(b) Single block grid generated for simulating flow over axisymmetric step.

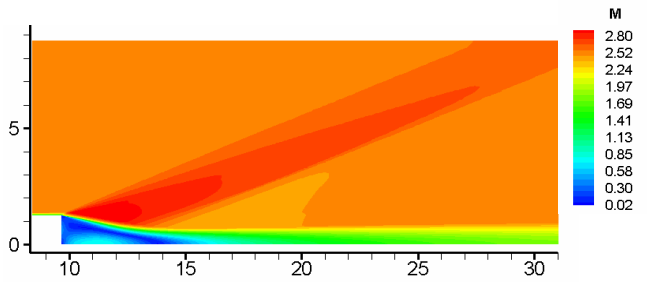

(c) Contours of Mach number, using k-ε model without compressibility correction.

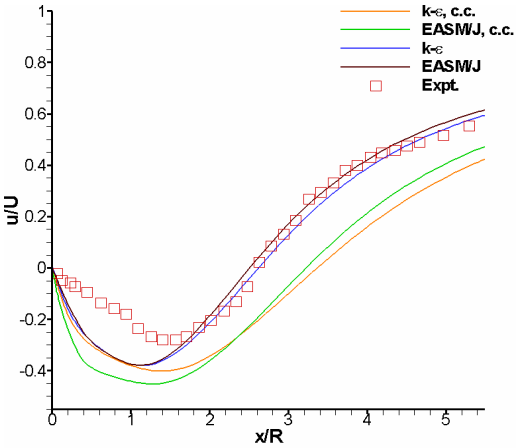

(d) Comparison of axial velocity distribution with experimental data of Herrin and Dutton [7].

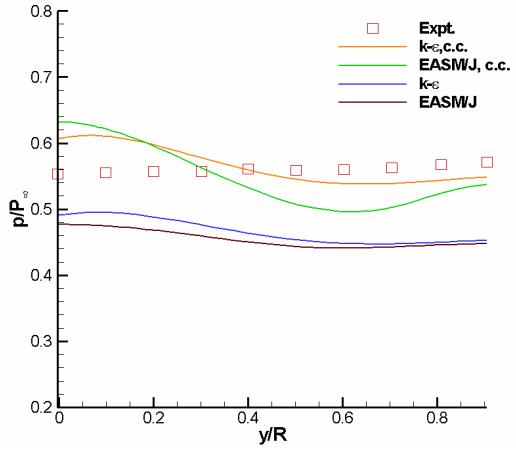

(e) Comparison of of base pressure distribution with experimental data of Herrin and Dutton [7].

Figure 2. Supersonic flow over axisymmetric step.

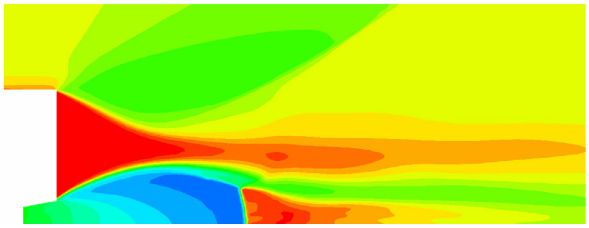

(a) Contours of Temperature.

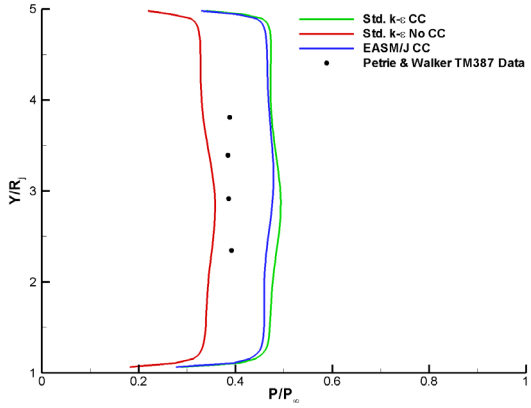

(b) Comparison of base pressure distribution with experimental data of Petrie and Walker[8].

Figure 3. Propulsive jet with base region results[23].

C. Lateral Slot Jet Study

A sonic, underexpanded, gaseous jet from a transverse slot issuing into a supersonic external flow is the object of this study, with the data of Spaid and Zukoski [9] used for comparisons. The slot jet stream consists of nitrogen gas, and the external stream is air at Mach number 3.5. The underexpanded jet penetrates into the external stream, is turned by the momentum of the external stream, and it obstructs the external flow producing a shock that causes the boundary layer to separate. The shock/boundary layer interaction upstream of the step plays significant role in this problem, and it is found that the separation zone ahead of the jet is strongly influenced by compressibility effects. Performing a preliminary analysis using EASM/J, the surface pressure distribution is compared with the results predicted using k-ε model by Papp at al. [4] in Figure 4. For this analysis, compressibility correction was not used with EASM/J, and the trend of the pressure distribution obtained with EASM/J is comparable with the surface pressure distribution obtained with k-ε model, without the correction. Using the compressibility correction, the size of the upstream separated region is substantially larger and compares well with data. For a similar problem with a helium jet, comparisons obtained with compressibility correction were not as good [13].

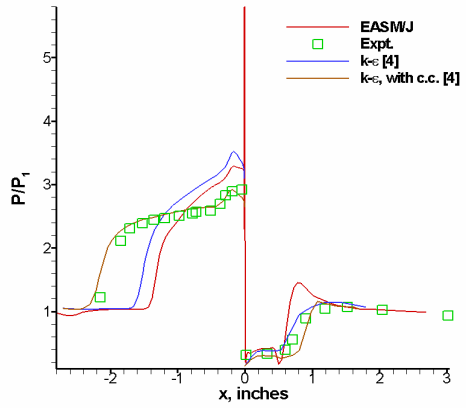

Figure 4. Comparison of base pressure distribution with experimental data of Spaid and Zukoski[9].

D. Propulsive Jet with Lobes Study

Earlier studies of passive noise reduction concepts for military aircraft involved the use of chevrons, and micro-jets [10]. However, the amount of reduction in noise achieved was not large relative to the observed drop in the engine performance. A recent and novel concept of 'corrugated nozzle' has been designed at NCPA/U. MISS, and the numerical simulations for this corrugated nozzle concept [1], are discussed in this section. These corrugations are lobes installed into the divergent portion of the nozzle, and extend from the throat to the exit of the nozzle. The exit views of a baseline nozzle, and a nozzle installed with 6-lobes are shown in Figure 5. The presence of lobes in the nozzle, promotes strong streamwise vorticity in the developing jet region, and thereby enhances mixing of the jet flow with the surrounding freestream flow. Numerical simulation of the six-lobed nozzle has been performed using k-ε model turbulence model. For better prediction of the turbulent flow structure, and to assess the ability of EASM/J in fulfilling this objective, EASM/J analysis was also performed.

Subsonic flow has been prescribed at the inflow boundary specifying total pressure, P_o, and total temperature, T_o. Non-reflecting boundary condition is specified on the outflow boundary, where the flow variables extrapolated from

the interior by letting the first-order derivatives of all the flow variables normal to the boundary to vanish. The viscous walls are treated using compressible wall function approach, available in CRAFT CFD®. On the farfield boundaries, freestream boundary conditions are specified, allowing for entrainment of the jet. Assuming symmetry, the simulation has been performed for a half-corrugation.

The baseline k-ε model used can adequately address the mean flow effects of turbulent structures but cannot portray the Reynolds normal stress anisotropy observed in laboratory jets. EASM has the ability to better resolve turbulent flow structures in complex vortical flows compared to the basic k-ε model. This is an outcome of its development to satisfy turbulence realizability constraints and results in local modifications to Cμ based on the mean flow strain and vorticity behavior. This is shown more clearly by the turbulent kinetic energy contours along each of the jet symmetry planes in Figures 6 and 7. In the immediate vicinity of the nozzle lip, velocity strain values are significant, and the EASM is observed to predict lower turbulent levels in this region, which is felt to be more realistic. Since the developing region is finite and affected by upstream conditions, such small modeling details can impact downstream flow behavior until self-similarity is achieved.

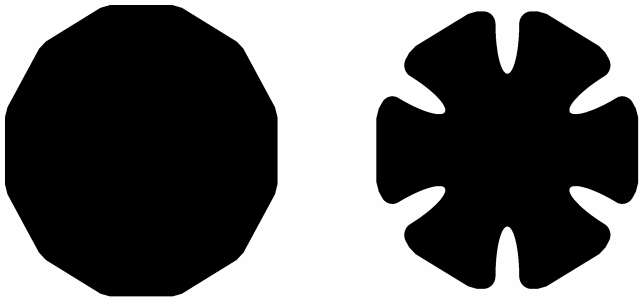

Figure 5. Nozzle exit plan forms of laboratory-scale F/A-18 nozzle with and without corrugations.

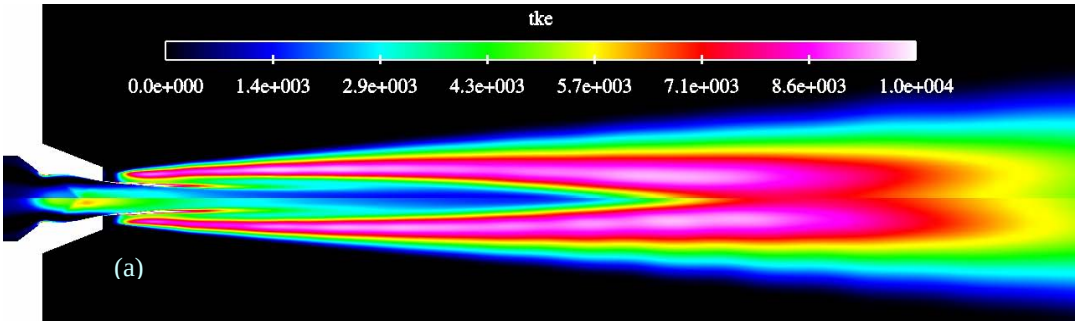

Figure 6. Turbulent kinetic energy contours showing reductions for 6-lobe nozzle with EASM/J (bottom half) and without EASM/J (top half): (a) in plane of lobes.

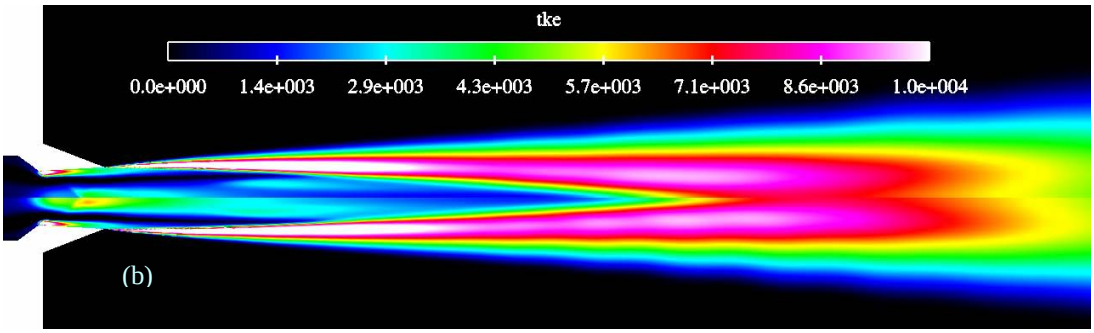

Figure 7. Turbulent kinetic energy contours showing reductions for 6-lobe nozzle with EASM/J (bottom half) and without EASM/J (top half):(b) symmetry plane between lobes.

E. Dual-Jet Interaction Study

In the present study, flow through a twin-jet nozzle at overexpanded flow conditions has been simulated to fulfill two objectives. Firstly, to study the effect of plenum design on the quality of flow at the nozzle exit. Secondly, to study the flow features of jet alone. Following the first phase, we observed that the flow is quite non-uniform as it reaches the nozzle exit, and the plenum design was modified to provide a much more uniform flow. Only the details of second phase of the simulation for nearly uniform flow nozzle exit plane conditions are discussed in the paper.

Subsonic flow has been prescribed at the inflow boundary specifying total pressure, P_o, which corresponds to NPR (Nozzle Pressure Ratio) = 3.94; and total temperature, T_o = 1022K. Non-reflecting boundary condition is specified on the outflow boundary, and viscous walls are treated using compressible wall function approach. On the farfield boundaries, freestream boundary conditions are specified, allowing for entrainment of the jet.

The key features of the supersonic jet issuing from the nozzle into still air are shown in Mach number contours of Figure 8. The jet is overexpanded, and a Mach disk occurs at approximately one diameter downstream, across which the supersonic flow became subsonic. The shear layers emanating from the lip of the nozzle merge at approximately 20 diameters downstream, which forms the end of potential core. This region is marked by a peak in the turbulent kinetic energy levels, as observed in the centerline variation of turbulent kinetic energy in Figure 9. To get a better understanding of the turbulence structure, the Reynolds normal stresses are plotted in Figures 10-12. Major part of the energy exchange from the mean flow to the turbulence is observed to occur through the streamwise Reynolds normal stress. Unlike the isotropic Reynolds normal stresses predicted using k-ε model, there are large differences in the values of the normal stresses predicted with EASM/J. This is a characteristic feature of EASM/J as it accounts for non-isotropy in the evolution of stresses via non-linear polynomial tensor representation of Reynolds stresses. The EASM/J calculations are felt to be more realistic and results will be validated by upcoming experiments at FSU by Krothapalli and coworkers.

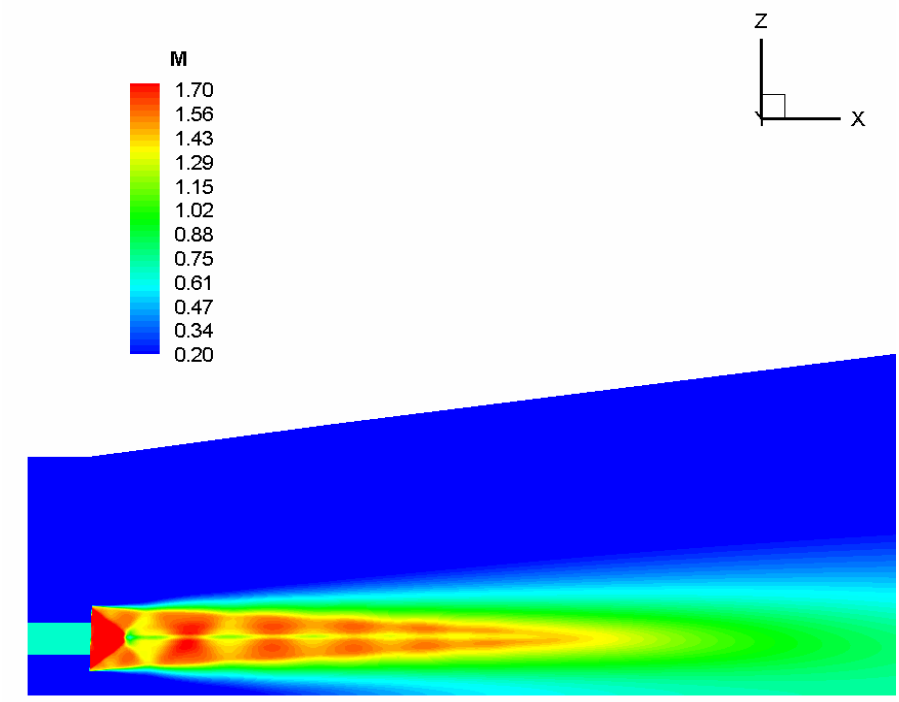

Figure 8. Mach number contours, showing the flow structure predicted using k-ε model.

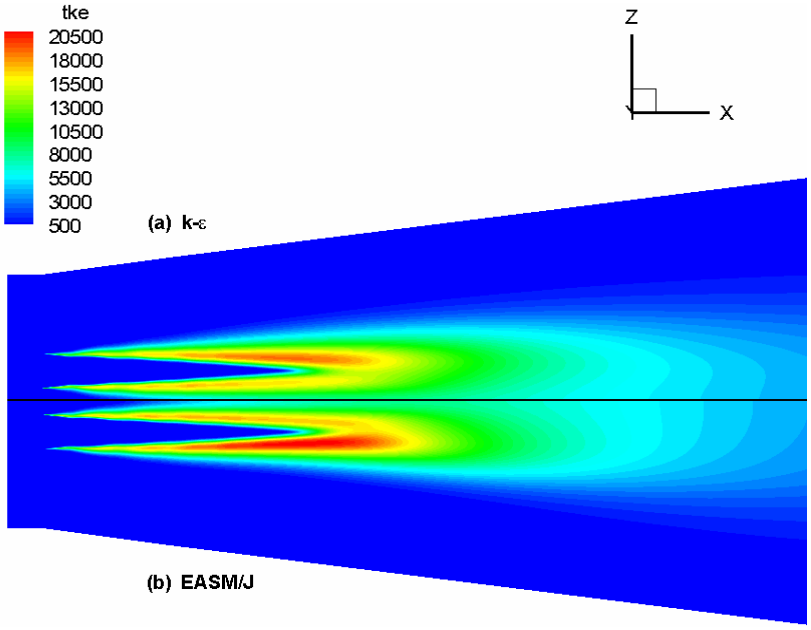

Figure 9. Turbulent kinetic energy contours obtained using (a) k-ε model (b) EASM/J model.

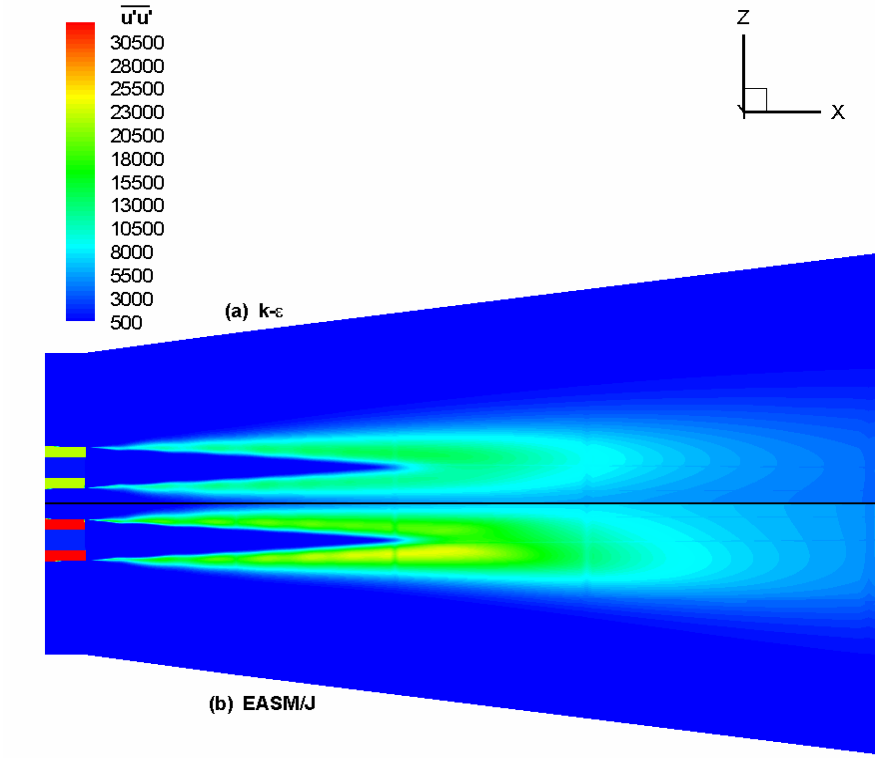

Figure 10. Streamwise Reynolds normal stress, $\overline{u'u'}$ contours obtained using (a) k-ε model (b) EASM/J model.

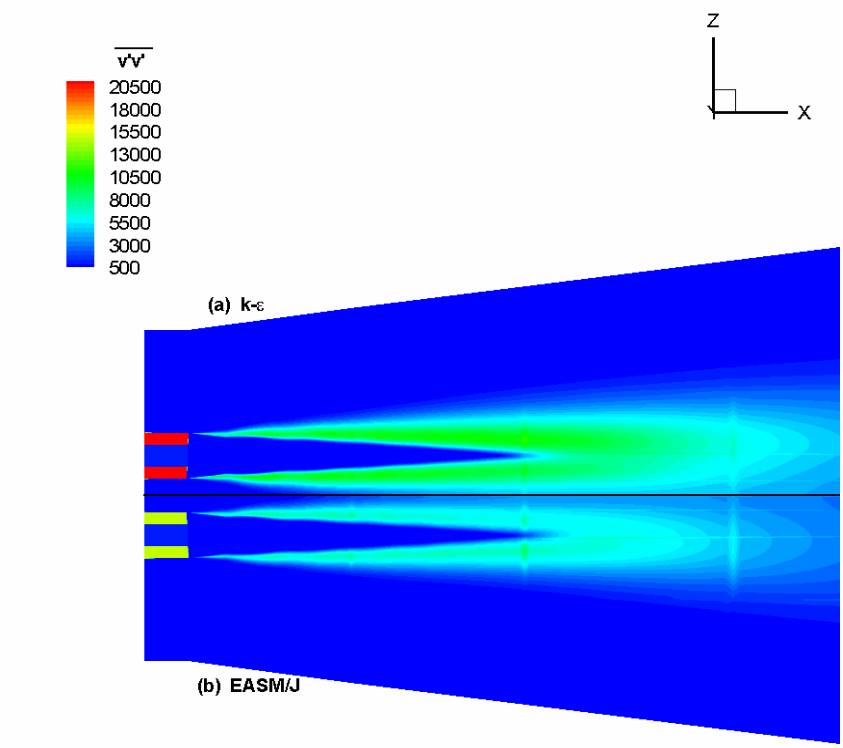

Figure 11. Transverse Reynolds normal stress contours, $\overline{v'v'}$ obtained using (a) k-ε model (b) EASM/J model.

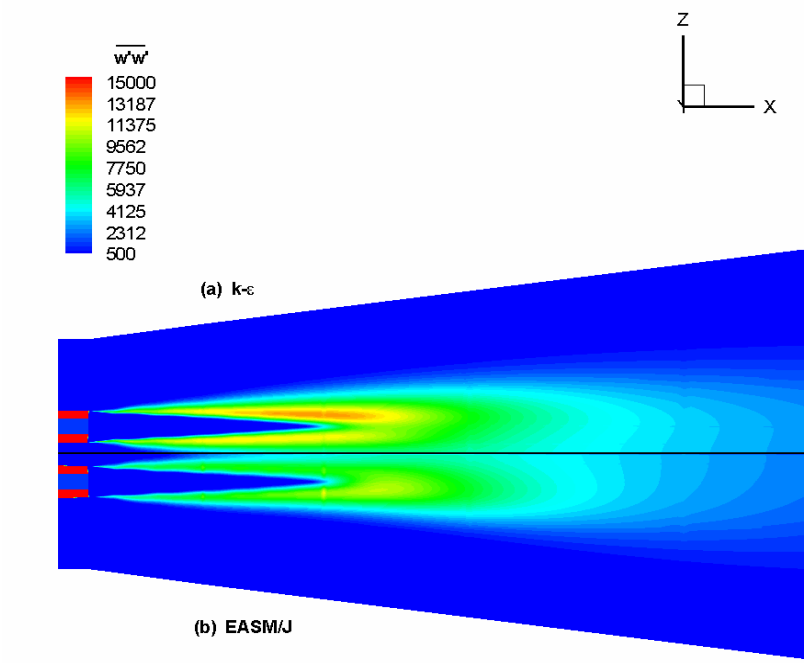

Figure 12. Spanwise Reynolds normal stress contours, $\overline{w'w'}$ obtained using (a) k-ε model (b) EASM/J model.

VII. Conclusions

The application of an explicit algebraic stress model and its usage with a turbulence compressibility correction for simulating complex aeropropulsive problems has been demonstrated using CRAFT CFD flow solver. EASM extends baseline k-ε framework, validated to yield correct mean flow mixing, for a variety of free shear flows, to account for non-uniform distributions in the Reynolds normal stresses and improved turbulence realizability for complex 3-D flows. Better comparisons are obtained for base pressure using a compressibility correction but at the expense of longer than experimentally observed reattachment lengths for base flows. Predicted streamwise velocity distributions within the recirculation zone are consistently higher than the measurements of Herrin and Dutton. For the lateral jet problem, improvements using compressibility correction were significant and yielded a separation zone size consistent with data. EASM/J has improved ability to resolve turbulent flow structures in complex vortical flows, compared to the k-ε model, as demonstrated by the lobes mixing study. The adequacy of the compressibility correction as implemented in CRAFT CFD to represent the flow features of high speed, compressible flows still needs further investigation. This requires improved modeling of the pressure dilatation term in the turbulent kinetic energy equation of the baseline k-ε model, and this would further improve the predictive capability of EASM/J. Extensions to the ε-equation for the problems described such as curvature correction could also improve comparisons with data.

VIII. Acknowledgements

Portions of this work were supported by NASA, Army and Navy programs.

References

[1] Kenzakowski, D. C., Kannepalli, C., Brinckman, K. W., "Computational Studies Supporting Concepts for Supersonic Jet Noise Reduction," AIAA Paper 2004-0518, 42nd Aerospace Sciences Meeting and Exhibit, Reno, Nevada, January 5-8, 2004.

[2] Papp, J. L., Kenzakowski, D. C., and Dash, S. M., "Calibration and Validation of EASM Turbulence Model for Jet Flowfields," AIAA Paper 2002-0855, 40th Aerospace Sciences Meeting and Exhibit, Reno, Nevada, January 14-17, 2002.

[3] Kenzakowski, D. C., Papp, J. L., and Dash, S. M., "Modeling Turbulence Anisotropy For Jet Noise Prediction," AIAA Paper 2002-0076, 40th Aerospace Sciences Meeting and Exhibit, Reno, Nevada, January 14-17, 2002.

[4] Papp, J. L. and Dash, S. M., "Turbulence Model Unification and Assessment for High-Speed Aeropropulsive flows," AIAA Paper 2001-0880, 39th Aerospace Sciences Meeting and Exhibit, Reno, Nevada, January 8-11, 2001.

[5] Launder, B. E., Morse, A., Rodi, W., and Spalding, D. B., "Prediction of Free Shear Flows – A Comparison of the Performance of Six Turbulence Models," *Free Turbulent shear Flows*, Vol. I – Conference Proceedings, NASA Langley, Hampton, Virginia, July 20-21, 1972.

[6] Kenzakowski, D. C. and Papp, J. L., "EASM/J Extensions and Evaluation for Jet Noise Prediction," AIAA Paper 2005-0419, 43rd Aerospace Sciences Meeting and Exhibit, Reno, Nevada, January 10-13, 2005.

[7] Herrin, J. L., and Dutton, J. C., "Supersonic Base Flow Experiments in the Near Wake of a Cylindrical Afterbody," *AIAA Journal*, Vol. 32, No. 1, January 1994.

[8] Walker, B. J., and Petrie, H. L., "Tactical Missile Flow Investigation," JANNAF 15th Exhaust Plume Technology Meeting, 1985.

[9] Spaid, F. W., and Zukoski, E. E., "A Study of the Interaction of Gaseous Jets from Transverse Slots with Supersonic External Flows", *AIAA Journal*, Vol. 6, No. 2, pp. 203-212, 1968.

[10] Dash, S.M., "Simulation of Laboratory Jets and Full Scale Exhaust Plumes," Invited Paper, Paper No. FEDSM2003-45056, 4th ASME_JSME Joint Fluids Engineering Conference, Honolulu, Hawaii, July 6-11, 2003.

[11] Dash, S. M., Sinha, N., Kenzakowski, D. C., Papp, J. L., Yellin, K. A., York, B. J., and DeMagistris, M., "Review of Modeling Advances for Rocket Plume and Divert Jet Simulation," 27th EPTS JANNAF Meeting, NASA Stennis, Mississippi, May 5-9, 2003.

[12] Ott, J., Kannepalli, C., Brinckman, K., and Dash, S. M., "Scramjet Propulsive Flowpath Prediction Improvements Using Recent Modeling Upgrades," AIAA Paper 2005-0432, 43rd Aerospace Sciences Meeting and Exhibit, Reno, Nevada, January 10-13, 2005.

[13] Brinckman, K., Kenzakowski, D. C., and Dash, S. M., "Progress in Practical Scalar Fluctuation Modeling for High- Speed Aeropropulsive Flows," AIAA Paper 2005-0508, 43rd Aerospace Sciences Meeting and Exhibit, Reno, Nevada, January 10-13, 2005.

[14] Rodi, "A New Algebraic Relation for Calculating the Reynolds Stresses," *Journal of Applied Mathematics and Mechanics ZAMM*, Vol. 56, T219-T221, 1976.

[15] Pope, S., "A More General Effective Viscosity Hypothesis," *AIAA Journal*, Vol. 72, pp. 331-340, 1975.

[16] Gatski, T. B., and Speziale, C. G., "On Explicit Algebraic Stress Models for Complex Turbulent Flows," *Journal of Fluid Mechanics*, Vol. 254, pp. 59-78, 1993.

[17] Jongen, T. and Gatski, T. B., "General Explicit Algebraic Stress Relations and Best Approximation for Three-dimensional Flows," *International Journal of Engineering Sciences*, 36, pp. 739-763, 1998.

[18] Gatski, T. B. and Jongen, T., "Nonlinear Eddy Viscosity and Algebraic Stress Models for Solving Complex Turbulent Flows," *Progress in Aerospace Sciences*, 36, pp. 655-682, 2000.

[19] Sarkar, S., Erlebacher, G., Hussaini, M. Y., and Kreiss, H. O., "The Analysis and Modeling of Dilatational Terms in Compressible Turbulence," *Journal of Fluid Mechanics*, Vol. 227, pp. 473-493, 1991.

[20] Zeman, O., "Dilatation dissipation: The Concept and Application in Modeling Compressible Mixing Layers," *Physics of Fluids A*, 2 (2), pp. 178-188, 1990.

[21] Zeman, O, "On the Decay of Compressible Isotropic Turbulence," *Physics of Fluids A*, 3 (5), pp. 951-955, 1991.

[22] So, R. M. C., Sarkar, S., Gerodimos, G., and Zhang, J., "A Dissipation Rate Equation for Low-Reynolds Number and Near-Wall Turbulence", *Theoretical Computational Fluid Dynamics*, Vol.9, pp. 47-63, 1991.

[23] Papp, J. L., Sinha, N., and Kenzakowski, D.C., "A Next Generation Engineering Axisymmetric Flowfield Model, RPFM for Plume and Hard Body Analysis," 28th EPTS and 10th SPIRITS User Group Joint Meeting, San Diego, California, November 1-5, 2004.